# USE OF MAGNESIAN-DOLOMITE MIXTURES IN STEEL-MELTING FURNACE HEARTHS AND THE MECHANISM OF THEIR WEAR IN SERVICE. 1. STUDY OF JEHEARTH REFRACTORY MIXTURE

**T. I. Shchekina,[1] E. N. Gramenitskii,[1] A. M. Batanova,[1] T. A. Kurbyko,[1] A. V. Likhodievskii,[1] B. N. Grigor'ev,[1] A. N. Pyrikov,[1] O. Sheshevichka,[2] and R. Gazhur[2]**

Translated from *Novye Ogneupory*, No. 12, pp. 31 – 41, December, 2006.

*Original article submitted August 23, 2006.*

The results of mineralogical-petrographic analysis of Jehearth magnesian-dolomite refractory mixture used in the hearths of steel-melting furnaces are described. The variation regularities of its phase and chemical composition are identified and the mechanism of its wear in service at the metallurgical works in Russia is considered.

The present study is the continuation of the preceding paper [1] and focuses on the refractory material Jehearth produced by the Slovakian Magnesite Works and used in the hearths of open-hearth furnaces at the Vyksunskii Metallurgical Works. We have also investigated the initial material, namely magnesian-dolomite mixture of grade Jehearth 30BA. Materials were studied using the methods of optical and electron microscopy, microprobe, silicate, and x-ray phase analysis described in [1].

## RESULTS OF INVESTIGATION AND DISCUSSION

The initial refractory mixture Jehearth 30 BA (sample M22) used in the post-blow zone of an open-hearth furnace has the form of a gray powder with a yellowish tint and prevailing particle size < 0.5 mm; the lateral size of 0.5 – 1.5 mm is observed in less than 30% particles. Around 7% of the mixture is represented by aggregate fragments or "lumps" of rounded or slightly elongated shape and size up to 10 mm. The largest of these fragments have a flattened shape resembling shingle. Petrographic analysis identifies these fragments as a typical granoblastic structure formed by isometric periclase grains of size ranging from 0.04 to 0.2 mm with rare pores of length 0.1 mm. The periclase grains have a hexagonal section with slightly rounded angles. According to the probe analysis data, periclase contains 4% wustite component with traces of Si, Al, Mn, Ca, K, and P. The interstices contain bands of size up to 0.1 – 0.3 mm identified as bicalcium silicate and a spinel-like phase whose composition is close to calcium ferrite.

The chemical composition of the initial refractory differs from its specifications [2] by a higher content (within 0.5 – 2 wt.%) of $SiO_2$, $Al_2O_3$, and CaO and a lower content of MgO and FeO + $Fe_2O_3$ (Table 1). Iron exists in the initial refractory mainly as the trivalent form. The CaO/SiO ratio found by silicate analysis is 1.7 times lower than the specifications data, due to a higher content of $SiO_2$.

According to the norm (Table 1) of the initial material, the quantitative ratio of its phases is as follows (mol.%): periclase 90.5, bicalcium silicate 2.1, bicalcium ferrite 5.4, and CaO 2.0.

Variations occurring in refractory Jehearth 30BA in service were studied on the basis of two samples taken from different parts of the furnace hearth: from the front bank at the level of the slag belt near the middle blow zone (M34) and from the back bank (M2).

Sample M34 of size 100 × 80 × 60 mm is monolithic and has a zonal structure. The sintered part of the sample, which is the remotest from the site of contact with molten metal and slag (over 55 mm), which is classified as the least altered zone 1, has a light gray color with a yellowish shade and a brecciated structure. The prevailing fragments are elongated light-colored yellowish periclase fragments of length from 1 to 5 mm cemented by a close-grained (0.03 – 0.15 mm) binding (main) mixture with a granoblastic structure (Fig. 1*a*). The fragment edges are frequently decorated by metal iron

[1] Lomonosov Moscow State University, "OgneuporTreidGrup" Co., Russia.
[2] Slovakian Magnesite Works, Slovakia.

formations of thickness from several fractions of a millimeter to 1 mm. The binding mixture contains 60% periclase grains and 40% tricalcium silicate, ferrous calcium spinellide phases, tricalcium aluminate, and a small quantity (a few percent) of lime (Table 2); calcium titanate is identified as well. All phases in the binder are newly formed, which is responsible for its sintering into a monolithic stone. A small quantity of narrow pores of length up to 0.1 mm are confined near the boundaries of the fragments and less frequently near the grains boundaries in the binding mixture.

Nearer to the contact with melts, the material of zone 1 acquires a darker gray tint. The content of the binding mixture grows due to the finest fragments of periclase aggregates whose angular edges becomes rounded. At a distance from 55 to 29 mm one observes variations in the microstructure of the zone (Fig. 1*b*). Periclase grain aggregates become zonal. At the edges of the aggregates new periclase grains are formed or recrystallized, as well as grains of silicates aluminates, and other phases. The recrystallized areas typically contain small elongated pores (5 × 20 μm) at the grain boundaries. The metal phase does not border the periclase aggregates, it is usually separated from them by a strip of the binding mixture. In this part of the zone, the content of aluminum, silicon, and calcium oxides perceptibly grows due to a decreased content of magnesium oxide, while the content of iron oxide persists at the same level. A small quantity of sulfur and titanium is observed. The substitution of periclase is manifested as a reaction edge of thickness 0.1 mm, which

**TABLE 1.** Gross Chemical Composition and Phase Norm of Initial Refractory Jeharth 30BA (Sample M22) and Zones of Interaction with Melts (Sample M34)

| Parameter | M34 (microprobe analysis) | | | | | | M34 (silicate analysis)*[1] | | | M22 (initial)*[2] |
|---|---|---|---|---|---|---|---|---|---|---|
| Zone | 4 | | 3 | 2 | 1 | | 3 (black-dark brown) | 2 (yellow-gray) | 1 (gray) | |
| Distance from contact with melt, mm | 0 – 0.6 | 0.6 – 4 | 4 – 6 | 6 – 14 | 14 – 45 | 45 – 85 | 0 – 6 | 6 – 14 | 14 – 85 | 0/0 |
| Mass content, %: | | | | | | | | | | |
| $SiO_2$ | 1.60 | 3.13 | 2.17 | 16.46 | 9.60 | 7.00 | 3.06 | 7.26 | 5.38 | 1.00/2.18 |
| $TiO_2$ | — | — | — | — | 0.27 | 0.30 | 0.05 | 0.30 | 0.19 | N.D./0.03 |
| $Al_2O_3$ | 0.76 | 0.53 | 0.70 | 1.21 | 4.39 | 4.70 | 0.30 | 4.94 | 5.88 | 0.30/0.69 |
| $Fe_2O_3$ | — | — | — | — | — | — | 41.67 | 0.35 | 0.50 | 4.51/2.10 |
| FeO | 83.84 | 85.29 | 42.07 | 15.70 | 5.56 | 7.75 | 24.15 | 10.08 | 8.96 | N.D./0.36 |
| MnO | 0.72 | 0.39 | 0.95 | 0.93 | 0.61 | 0.68 | 0.66 | 0.67 | 0.62 | » » /0.22 |
| MgO | 6.59 | 6.67 | 45.72 | 55.16 | 61.14 | 65.71 | 23.19 | 54.57 | 59.05 | 86.17/84.19 |
| CaO | 6.49 | 3.99 | 8.39 | 10.54 | 18.49 | 13.86 | 6.92 | 21.83 | 19.42 | 8.02/10.23 |
| $CaO/SiO_2$*[3] | 4.34 | 1.36 | 4.14 | 0.69 | 2.06 | 2.12 | 2.42 | 3.22 | 3.87 | 8.57/5.03 |
| Phase content (norm analysis), mol.%*[4]: | | | | | | | | | | |
| Per | — | — | — | — | 63.5 | 69.2 | — | — | — | 90.5/89.0 |
| FePer | — | — | 64.5 | 48.5 | — | — | 39.4 | 67.3 | 71.9 | —/— |
| $C_3S$ | — | — | — | — | — | — | — | 22.8 | 16.7 | —/— |
| $C_2S$ | — | — | 5.9 | — | — | — | — | — | — | 2.1/4.7 |
| $(C, M)_2S$ | 5.4 | 11.0 | — | 39.7 | 21.8 | 15.3 | 9.6 | — | — | —/— |
| $C_3A$ | — | — | — | — | — | — | — | — | — | —/— |
| $C_2A$ | — | — | — | — | 8.9 | 8.0 | — | 9.5 | 10.7 | —/— |
| $C_2F$ | 8.8 | — | 8.2 | — | — | — | 2.3 | — | — | 5.4/3.4 |
| $C_4AF$ | — | — | — | 4.6 | — | — | — | — | — | —/— |
| Mf | 34.7 | 28.2 | 21.4 | 7.2 | 5.3 | 7.1 | 47.1 | — | 0.4 | —/— |
| Ws | 20.9 | 16.7 | — | — | — | — | 1.5 | — | — | —/— |
| Mt | 30.2 | 44.1 | — | — | — | — | — | — | — | —/— |
| Prv | — | — | — | — | 0.4 | 0.4 | 0.1 | 0.4 | 0.3 | —/— |
| CaO | — | — | — | — | — | — | — | — | — | 2.0/2.9 |

*[1] Data from the GIN laboratory of the Russian Academy of Sciences.

*[2] Numerator — standard data, denominator — data from silicate analysis performed at GIN laboratory.

*[3] Molecular ratio.

*[4] Per — periclase MgO; FePer — ferrous periclase; $C_2S$ — tricalcium silicate $3CaO \cdot SiO_2$; $C_2S$ — bicalcium silicate $Ca_2SiO_4$; $(C, M)_2S$ — magnesium-bearing bicalcium silicate $(Ca, Mg)_2SiO_4$; $C_3A$ — tricalcium aluminate $3CaO \cdot Al_2O_3$; $C_2A$ — bicalcium aluminate $2CaO \cdot Al_2O_3$; $C_2F$ — bicalcium ferrite $2CaO \cdot Fe_2O_3$; $C_4AF$ — braunmillerite $4CaO \cdot Al_2O_3 \cdot Fe_2O_3$; Mf — magnesioferrite $MgFe_2O_4$; Ws — wustite FeO; Mt — magnetite $Fe_3O_4$; Prv — perovskite $CaTiO_3$; CaO — lime.

differs from the binding mixture by a finer-grained structure (0.02 against 0.06 mm). This border edge is located at the periphery of the fragments consisting of periclase aggregates. Calcium sulfide (oldhamite) is registered; spinellides and titanates are not identified. A small quantity of Ti is contained in silicates, Fe and Si are contained in calcium aluminate (Table 2), and Mg is contained in both phases. Grains of pure iron and silicon are occasionally found in the pores.

The boundary between zone 1 and zone 2, which is more perceptibly altered, is rather clearly visible in the sample due to the grayish-brown tint of the binding mixture, a decreased amount of fine yellowish fragments, and merging of dark gray spots with the main binding mixture. The boundary with the preceding zone is uneven, with numerous outcrops; accordingly, the thickness of this zone varies from 4 to 8 mm. The zone retains its initial brecciated structure. Periclase be-

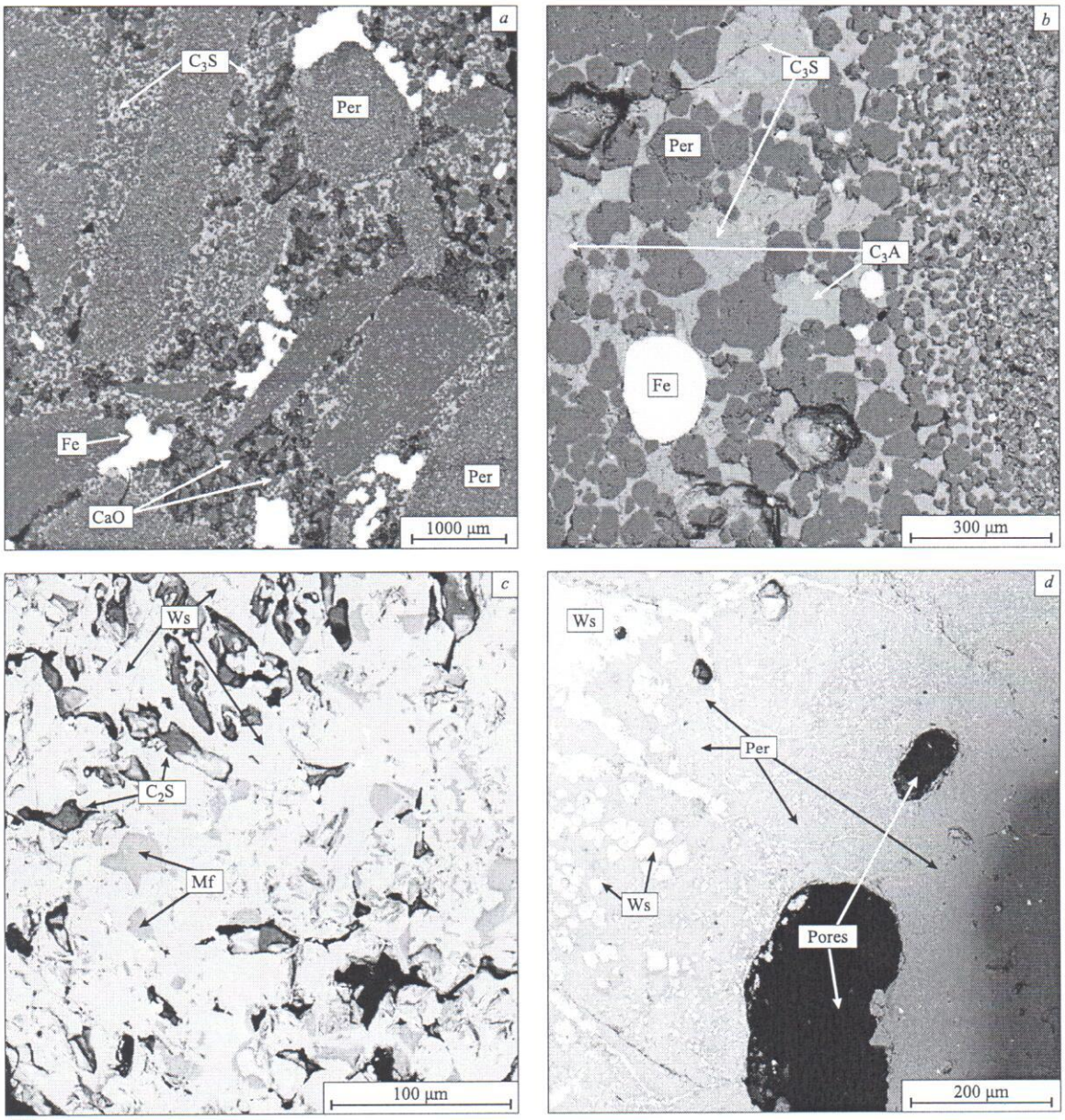


**Fig. 1.** Structure and phase composition of refractory Jeharth 30BA split by zones of sample M34 (backscattered electron image BSE on a CAMSCAN 4DV electron microscope): *a*, brecciated structure of sintered refractory mixture in zone 1; note the heterogeneity of the binding mixture and the periclase aggregate fragments bordered by metallic iron ; *b*, the border edge at the boundary of periclase aggregate fragments (right) with the binding mixture differing from it by a finer-grained structure and the formation of pores; *c*, structure of zone 4, which is nearest to the melt and contains wustite, magnesioferrite, and bicalcium silicate; *d*, dendrite- and veinlet-shaped wustite formations among ferrous periclase crystals and formation of large pores in zone 4.

comes more ferrous (Table 2). The phase composition of the binding mixture changes significantly. Instead of tricalcium silicate and aluminate, bicalcium silicate and braunmillerite are crystallized; calcium sulfide is not identified. The metallic iron phase is significantly smaller. Periclase acquires zonality. The ferrous coefficient $f = Fe/(Mg + Fe)$ in the relicts of the initial grains is 0.05, whereas in the recrystallized areas of the binder it reaches 0.26. Iron is permanently present in bicalcium silicate. The concentration of aluminum, on the contrary, decreases in this direction; Ti and Mg in this phase are registered in quantities close to or lower than the identification limits. Braunmillerite has a lower ratio of the sum of iron plus aluminum to calcium and of aluminum to iron than the theoretical ratio; its titanium impurity is perceptible. Perovskite is present in zone 2.

Zone 3 of thickness around 5 mm has a dark brown color, its brecciated structure is well visible in the sample and in the material microstructure, but it is here a relict structure. The sizes of the fragments decrease due to the corrosion of the binder, and the smallest fragments have disappeared. Pores of size up to 0.3×1.0 mm are formed. The gross chemical composition of this zone becomes less magnesium-bearing and more ferrous, and the share of trivalent iron increases. The quantity of the wustite component in the periclase grows. Other phases that are found in small quantities are calcium ferrite and bicalcium silicate of a nearly theoretical composition.

Directly on the border of the melt we see the intensely altered zone 4 (thickness around 4 mm) in the form of a black crust. (Fig. 1*c*). Any relicts of the brecciated structure are totally absent. Four subzones can be discriminated in the cross-section of this zone. They differ in their structural specifics and quantitative phase ratios, but the set and composition of the phases is the same in all four subzones. Table 1 lists the gross compositions of two subzones. Within zone 4 we see especially many pores; some of them merge into cavities reaching 15 mm long and 3 mm wide. At least 90% of the crust material consists only of Mg and Fe oxides. Apart from those, only bicalcium silicate and rare grains of bicalcium ferrite are found. Both minerals contain a MgO

**TABLE 2.** Crystallochemical Formulas of the Phases of Refractory Mixture Jehearth 30BA in the Initial Sample (M22) and in Zones Formed after Service (Sample M34) Based on Microprobe Data

| Sample | Zone | *l*, mm | Phase*[1] | *f**[2] | Phase composition |
|---|---|---|---|---|---|
| M22 | 0 | > 85 | Per | 0.04 | $(Mg_{0.95}Fe_{0.04})_{0.99}O$ |
| | | | $C_2S$ | | $(Ca_{1.97}Mg_{0.11})_{2.08}(Si_{0.92}Fe_{0.02}P_{0.01}))_{0.95}O_4$ |
| | | | $C_2F$ | | $(Ca_{2.25}Mg_{0.06}Mn_{0.05})_{2.36}(Fe_{1.53}Al_{0.34}Ti_{0.02}Si_{0.28})_{2.17}O_5$ |
| M34 | 1 (gray) | 85 – 45 | Per | 0.0 | $(Mg_{0.99}Mn_{0.01})_1O$ |
| | | | $C_3A$ | | $(Ca_{2.92}Mg_{0.01}Mn_{0.01})_{2.97}(Al_{1.79}Ti_{0.01}Si_{0.16})_{1.96}O_6$ |
| | | | $C_3S$ | | $(Ca_{2.89}Mg_{0.08})_{2.97}(Si_{0.96}Ti_{0.01}Al_{0.04})_{1.01}O_5$ |
| | | | Fe | | $(Fe_{0.84}Mn_{0.01}Si_{0.14})_{0.99}$ |
| | | | Prv | | $(Ca_{1.11}Mg_{0.06})_{1.17}(Ti_{0.49}Al_{0.44}Si_{0.07})_1O_3$ |
| M34 | | 45 – 14 | Per | 0.0 | $(Mg_{0.98}Ca_{0.01}Mn_{0.01})_1O$ |
| | | | $C_3A$ | | $(Ca_{2.92}Mg_{0.03})_{2.05}(Al_{1.82}Fe_{0.01}Si_{0.14})_{1.97}O_6$ |
| | | | $C_3S$ | | $(Ca_{2.95}Mg_{0.07})_{3.07}(Si_{0.96}Ti_{0.01}Al_{0.03})_1O_5$ |
| | | | $C_2S$ | | $(Ca_{0.98}Mg_{0.02})_1SO_4$ |
| | | | Fe | | $(Fe_{0.99}Mn_{0.01})_1$ |
| M34 | 2 (yellow-gray) | 14 – 9 | FePer | 0.20 | $(Mg_{0.78}Ca_{0.01}Mn_{0.01}Fe_{0.20})_1O$ |
| | | | $C_2S$ | | $Ca_{2.08}(Si_{0.92}Fe_{0.03}Cr_{0.02}Ti_{0.01})_1O_4$ |
| | | | $C_4AF$ | | $(Ca_{4.49}Mg_{0.09}Mn_{0.03})_{4.61}(Al_{1.31}Ti_{0.21})_{1.52}(Fe_{2.74}Si_{0.12})_{2.86}O_{10}$ |
| | | 9 – 6 | FePer | 0.22 | $(Mg_{0.77}Mn_{0.01}Fe_{0.22})_1O$ |
| | | | $C_2S$ | | $(Ca_{2.05}Mg_{0.01})_{2.06}Si_{0.97}O_4$ |
| | | | $C_2F$ | | $Ca_{2.42}(Fe_{2.16}Al_{0.16}Ti_{0.01}Si_{0.06})_{2.39}O_5$ |
| M34 | 3 (grayish-brown) | 6 – 4 | FePer | 0.27 | $(Mg_{0.72}Mn_{0.01}Fe_{0.27})_1O$ |
| | | | $Ca_2F$ | | $(Ca_{2.36}Mg_{0.05}Mn_{0.01})_{2.42}(Fe_{2.07}Al_{0.15}Ti_{0.04}Si_{0.09})_{2.35}O_5$ |
| | | | $C_2S$ | | $(Ca_{1.86}Mg_{0.20})_{2.06}(Si_{0.89}Fe_{0.14}Cr_{0.02})_{1.05}O_4$ |
| M34 | 4 (black) | 4 – 0.6 | Ws | 0.91 | $(Fe_{0.88}Mg_{0.09}Ca_{0.01}Al_{0.01})_1O$ |
| | | | $C_2S$ | | $(Ca_{1.50}Mg_{0.24}Fe_{0.32})_{2.06}(Si_{0.93}P_{0.01})_{0.94}O_4$ |
| | | | FePer | 0.68 | $(Fe_{0.67}Mg_{0.31}Mn_{0.01})_{0.99}O$ |
| | | | Mf | | $(Mg_{0.88}Mn_{0.01}Ca_{0.04})_{0.96}Fe_{3.04}O_4$ |
| | | | (C, M)2F | | $(Ca_{1.08}Mg_{0.30}Mn_{0.01}Fe_{1.12})_{2.51}Fe_{2.50}O_5$ |

*[1] Fe — iron alloy; $(C, M_2)F$ — Mg-bearing calcium ferrite $2(Ca, Mg)O \cdot Fe_2O_3$.

*[2] *f*— ferrous coefficient Fe/(Fe + Mg).

impurity. According to silicate analysis data (Table 1), iron in zone 3 exists both in bivalent and trivalent forms (Table 2) with the weight ratio $Fe_2O/FeO = 1.71$. The most ferrous of the two coexistent phases identified by electron microscopy and microprobe analysis (Table 2) in all four subzones has a constant ferrous coefficient equal to 0.91. The composition of this phase well agrees with the formula of magnesiowustite. If this phase contains only bivalent iron, then at 1570°C and higher it can exist only as a melt [3], whose participation in steel melting processes has been reported in the literature [4]. The formation of wustite veinlets at the boundary with zone 3 and the dendrite shape indirectly support this assumption (Fig. 1*d*). The second ferrous phase has an unstable composition. It contains 64 – 78% wustite component converted to the periclase solid solution. According to the phase diagram, the coefficient $f$ of magnesiowustite that everywhere coexists with the melt should be close to the upper limit of this interval. The electron microscopy data (Fig. 1*c*) and microprobe analysis (Table 2) indicate the presence of another magnesian-ferrous phase, in addition to magnesiowustite. The formation of magnesioferrite is the most probable, which is corroborated by the high magnetization of the crust. The iron fraction in the sum of iron and magnesium is close to the theoretical value of 67%. The high content of trivalent iron as well corroborates the inevitability of the formation of spinellides of the magnesioferrite-magnetite group in zone 4. Their presence is confirmed by the data of x-ray phase analysis. Trivalent iron is also contained in Mg-bearing nonstoichiometric calcium ferrite.

The norm of zones 3 and 4, taking into account the quantitative ratio of bi- and trivalent iron in the refractory, includes wustite, magnesioferrite, magnetite, bicalcium silicate, and bicalcium ferrite. According to the phase diagram of the $MgO–FeO–Fe_2O_3$ system [5], magnesioferrite and magnetite at 1400 – 1600°C form a continuous series of solid solutions. The figurative point of zone 4 in this system lies in the field of coexistence of magnesioferrite + magnesiowustite + liquid, which suggests that these two minerals in zone 4 crystallize from the melt.

The variation in the gross composition of sample M32 along the zones depending on the distance to the contact with the melt is indicated in Fig. 2. This diagram correlates the atomic quantities of the elements (per 1600 oxygen atoms, the Bart method) ranging from the initial refractory in zone 0 to the composition of zone 4 (the nearest to the melt).

The most significant feature on the boundary between zones 1 and 2 is the removal of magnesia, which is more perceptible approaching zone 3. A small contribution of Si and Mn oxides and a more substantial contribution of Fe is observed. The maximum contents of Ca and Al caused by the removal of magnesia are registered at a distance of 30 – 50 mm from the contact. Their concentrations become lower in zone 3. Aluminum and calcium make up part of tricalcium aluminate in zone 1 and braunmillerite in zone 2. Besides, calcium is also contained in the silicates and ferrites. On the other hand, the content of Fe oxides at the boundary between zones 3 and 4

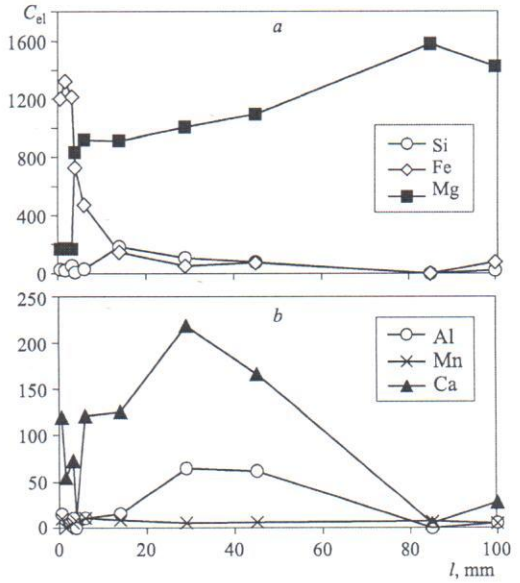


**Fig. 2.** Variations in the gross composition of elements ($C_{el}$, atomic quantities per 1600 atoms of oxygen) along the zones of sample M34 depending on the distance $l$ from non-altered refractory Jehearth 30BA (the point is arbitrarily set at 100 mm) to the contact with the melt (point 0): *a*, Si, Fe, Mg; *b*, Al, Mn, Ca.

sharply grows, while the content of Mg oxide is nearly constant. The intense contribution of Fe oxide is related to the variation in the phase composition on the boundary between zones 2 and 3 and between zone 3 and 4. The content of Ca grows again in zone 4, which is presumably related to its contribution from melted slag. Not only the quantities of iron (II) and (III) oxides, but their ratio as well, vary along the zones. Whereas iron in the initial material is present in a small quantity and mainly as the trivalent form, after service its quantity grows to 8 – 15 wt.% in the first two zones with perceptible prevalence of the bivalent form. It is mainly found in periclase. The content of iron in zones 3 and 4 grows to 40 – 85 wt.%, and its trivalent form clearly starts prevailing, which is manifested in the formation of magnesioferrite and calcium ferrites in addition to magnesiowustite (Table 1). This indicates a change in the redox conditions throughout the phases.

The second sample investigated in detail (M2) was taken from another spot: the back bank of the furnace hearth. This sample as well has experienced intense transformation with clearly expressed zonality (Fig. 3*a*). Similarly to the previous case, the initial material of sample M2 is mixture Jehearth 30BA [2]. The interaction between the refractory and metallurgical slag is similar to the interaction revealed in sample M34, but has some peculiarities. The total thickness of the zones comprises 35 mm. The variations in the gross chemical composition and the phase norm of the material across the hearth zones depending on the distance from the contact with metallurgical slag can be traced in Table 3; the crystal-che-

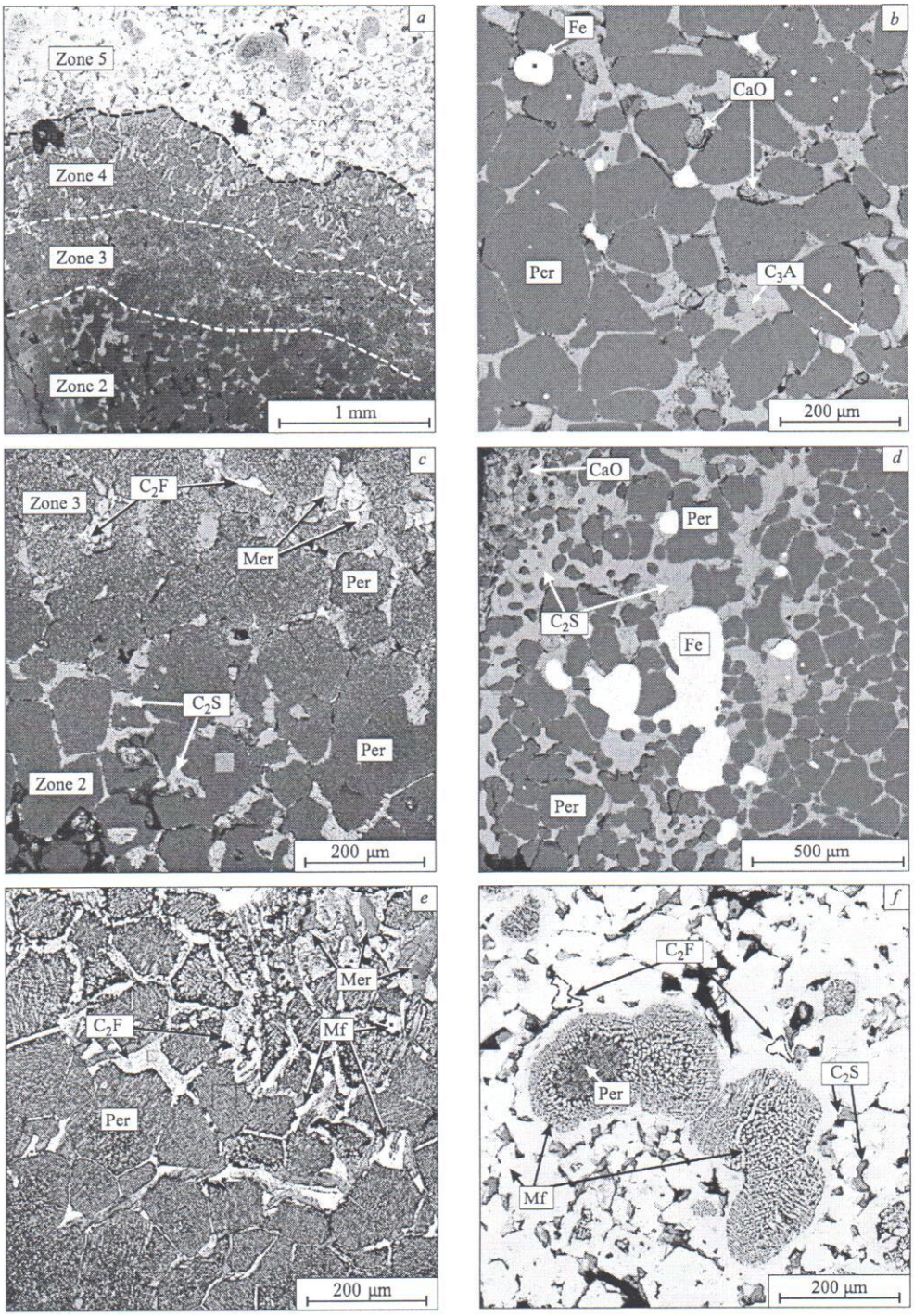


**Fig. 3.** Variations in the phase composition and structure split by zones for the refractory Jeharth 30BA in sample M2: *a*, zonal structure of the sample, general view, BSE image; *b*, structure of the least altered zone 1 consisting of periclase and the binder represented by tricalcium aluminate; lime formations and metal phase inclusions are visible; *c*, changes in the phase composition of the refractory at the zone boundary: the binder materials in zone 2 is bicalcium silicate and in zone 3 — mervinite and calcium ferrite; *d*, metal phase formation in the binder of zone 2 with the center rich in siliceous iron; *e*, formation of magnesioferrite dendrites in periclase, change in the composition of the binder consisting of mervinite, calcium ferrite, and magnesioferrite passing from zone 3 to zone 4; *f*, typical structure of zone 5. Periclase is present in the form of relict grains replaced by magnesioferrite crystals; the spaces between the latter are filled by bicalcium silicate.

mical formulas of the phases is given in Table 4. Below we give brief mineralogical-petrographic characteristics of the sample zones.

Zone 1 is gray-colored, around 20 mm thick, and, similarly to sample M34, has a brecciated structure and consists of virtually pure periclase with small impurities of Fe, Mn, and Ti (Fig. 3*b*). The binding material is mainly represented by tricalcium aluminate, but in contrast to sample M34, about 20% is lime CaO (with Mg, Si, Fe, Mn impurities) replaced by portlandite $Ca(OH)_2$. These calcium phases are loose mixtures filling the pores. Rounded formations of metallic Fe whose size ranges from a few fractions of a millimeter to 40 mm with small inclusions of silicon-bearing Fe are found inside periclase grains and in the binding materials x-ray phase analysis registers small quantities of bicalcium silicate. According to the norm calculation, the content of periclase in zone 1 decreases from 90% in the initial mixture to 84%; the quantity of bicalcium silicate grows; tricalcium aluminate and magnesioferrite are formed. Magnesioferrite is not registered by microprobe analysis.

In zone 2 (15 – 10 mm from the contact), light brown periclase remains the main mineral with a slightly higher content of iron ($f = 0.03$). Finest magnesioferrite inclusions are found in it. However, the cementing mineral here is not tricalcium aluminate but bicalcium silicate (Fig. 3*c*). A similar composition of zone 2 is observed in sample M34 as well. The difference consists in the fact that the binding mixture here, similarly to zone 1, contains Ca-bearing phases in the form of loose material. There are metallic formations with coil-shaped contours in periclase grains (Fig. 3*d*). In the norm the quantity of periclase decreases compared to zone 2, the content of bicalcium silicate and tricalcium aluminate grows, and tricalcium ferrite appears.

In zone 3 (10 – 8.5 mm from the contact) magnesioferrite inclusions in periclase grains become larger, more textured, and form oriented thin lamellae. Instead of bicalcium silicate, the binder here is mervinite, which has not been identified in the analogous zone of sample M43 (zone 3) where braunmillerite has been formed. Mervinite contains Ti, Al, and Fe impurities, and calcium ferrite is formed in small quantities. The ferrous factor of periclase is nearly doubled ($f = 0.04 \div 0.06$), although remaining relatively low. The norm of the zone confirms the decreased content of periclase, the increase content of magnesioferrite, and the emergence of mervinite.

Zone 4 (8.5 – 7 mm from the contact) differs sharply from zone 3 by its dark brown color; its mineral composition significantly changes toward an increasing quantity of magnesioferrite and the formation of Mg-bearing calcium ferrite. Mervinite persists in this zone, but in a smaller quantity. Periclase becomes much more ferrous ($f = 0.23$). The structure varies significantly (Fig. 3*d*): the edges of periclase crystals are rounded; magnesioferrite formations in them acquire a dendrite shape or the shape of thin lamellae intersecting at a right angle; part of magnesioferrite is formed in spaces between the periclase crystals, forming edges of width up to 10 – 15 μm and length 100 μm; numerous Mg-bearing bicalcium ferrite formations are registered. Toward zone 5 these phases become larger and separate the periclase grains by wider strips. The quantitative composition of this zone is as follows: periclase 70 – 75%, the remaining 25 – 30% is nearly equally split between mervinite, magnesioferrite, and bicalcium ferrite. In the norm we observe a further decrease in the amount of periclase (to 60%) and its increasing wustite component ($f = 0.2$), as well as increasing content of magnesioferrite and the presence of mervinite.

Zone 5, which is the nearest to the contact with the melt (7 – 0 mm), is of macroscopically black color, separated by a well-visible boundary from the preceding zone 4 (Fig. 3*a*). Magnesioferrite and magnesiowustite prevail in its composition (70 – 80%), Periclase with a high ferrous factor ($f = 0.25 \div 0.36$) comprises about 10% and exists in the form of relict grains replaced by magnesioferrite inside the grains and along their periphery. Periclase grains are bordered by a magnesioferrite border (30 – 50 μm) that has a cellular and banded porous structure, which on the periphery is replaced by a smooth shell also made up of *Mf*. The major part of

**TABLE 3.** Gross Chemical Composition and Phase Norm of Refractory Jeharth 30BA Split by Zones in Sample M2 Based on Microprobe Analysis

| Parameter | Zone | | | | |
|---|---|---|---|---|---|
| | 5 | 4 | 3 | 2 | 1 |
| *l*, mm | 0 – 5 | 5 – 8.5 | 8.5 – 10 | 10 – 15 | 135 |
| Mass content, %: | | | | | |
| $SiO_2$ | 2.49 | 2.40 | 8.21 | 4.97 | 1.78 |
| $TiO_2$ | 0.09 | 0.03 | 0.27 | 0.47 | 0.45 |
| $Al_2O_3$ | 1.79 | 1.24 | 1.40 | 4.52 | 4.89 |
| $Fe_2O_3$ | | | | | |
| FeO | 66.45 | 34.49 | 9.46 | 5.28 | 3.17 |
| MnO | 1.47 | 1.41 | 1.14 | 1.04 | 0.45 |
| MgO | 22.19 | 56.12 | 70.10 | 56.87 | 80.64 |
| CaO | 5.36 | 4.31 | 9.42 | 26.85 | 8.62 |
| $CaO/SiO_2$ | 2.31 | 1.92 | 1.23 | 5.79 | 5.18 |
| Phase content (norm), mol.%: | | | | | |
| Per | | | 70.5 | 65.5 | 84.09 |
| FePer | 10.2 | 61.3 | | | |
| $(C, M)_2S$ | 7.5 | | 3.0 | 11.6 | 3.85 |
| Mer*2 | | 5.9 | 14.8 | | |
| $C_3S$ | | | | 10.2 | 6.20 |
| Mf | 78.0 | 32.0 | 10.8 | | 5.35 |
| $(C, M)_2F$ | 4.3 | +*1 | + | | |
| $C_3F$*2 | | | | 10.2 | |
| Per | | | 0.9 | 0.5 | 0.51 |
| CaO | | 0.8 | | 2.0 | + |

*1 Sign + means that the specified phase is registered in the zone using a microprobe.

*2 Mer — mervinite $Ca_3MgSi_2O_8$, $C_3F$ — tricalcium ferrite $3CaO \cdot Fe_2O_3$.

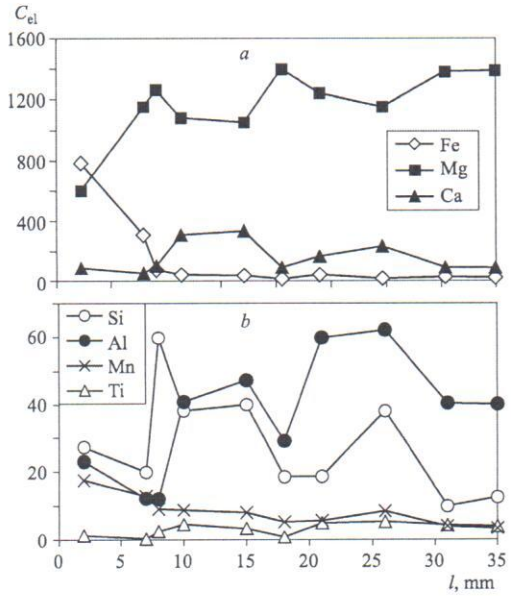


**Fig. 4.** Variations in the gross composition of elements along the zones depending on the distance from non-altered refractory Jehearth 30BA (the point corresponds to 35 mm) to the contact with the melt (point 0) in sample M2: *a*, Fe, Mg, Ca; *b*, Si, Al, Mn, Ti.

magnesioferrite forms crystals with a hexagonal or triangular section. Calcium-rich magnesioferrite is present as well in the form of small sites. Magnesioferrite, of all ferrous compounds, perceptibly prevails in zone 5, as distinct from the same zone in sample M34 where wustite comprises nearly half of the ferrous oxide phases. Bicalcium silicate is formed in spaces between magnesioferrite crystals in the form of xenomorphic formations of size up to 20 μm in the amount of ~10%. The content of magnesioferrite in the norm reaches 80%, the content of magnesiowustite 10%, and bicalcium silicate 7.5%.

The behavior of the main elements in refractory materials can be observed in Fig. 4. The elemental concentration curves have a complex form with segments of gradual or abrupt variations. At the beginning of zone 1, for ~10 mm we see no perceptible changes with respect to the initial refractory, which is arbitrarily set at a distance of 35 m. Later on, a decrease in magnesium content and increase in Ca, Si, and Al content begins, while the content of iron remains relatively low and constant. As a consequence, tricalcium aluminate emerges as the binding mineral.

In zone 2 (at a distance of 15 – 10 mm) the content of magnesium decreases rather sharply and, accordingly, the content of Ca and Si increases (the effect of their sum converted to 100% is presumably manifested as well). The binding mineral here is bicalcium silicate. The content of iron oxides increases, but only slightly.

Starting with zone 3, the concentrations of calcium and aluminum significantly decrease and the content of magnesium, silicon and, most important, iron grows. There is a deficit of calcium and as a consequence, mervinite is formed instead of bicalcium silicate. The increased content of Fe raises the ferrous factor of periclase and facilitates the formation of calcium ferrites.

**TABLE 4.** Crystalochemical Formulas of Phases of Refractory Mixtures Jeharth 30BA Split by Zones after Service (Sample M2)

| Zone | *l*, mm | Phase | *f* | Phase composition |
|---|---|---|---|---|
| 1 | 35 – 15 | Per | 0,01 | $(Mg_{0,98}Fe_{0,01}Ca_{0,01})O$ |
| | | $C_3A$ | | $(Ca_{2,88}Mg_{0,35})_{3,23}(Al_{1,75}Si_{0,17}Fe_{0,01}Ti_{0,04})_{1,97}O$ |
| | | CaO | | $(Ca_{0,42}Mg_{0,19}Fe_{0,01}A_{10,01}Mn_{0,02}Na_{0,004})_{0,65}O$ |
| | | Prv | | $(Ca_{1,12}Mg_{0,07})_{1,19}(Ti_{0,50}A_{10,45}Fe_{0,01}Si_{0,07}V_{0,01})_{1,04}O$ |
| 2 | 15 – 10 | Per | 0,03 | $(Mg_{0,97}Fe_{0,03})_{1,00}O$ |
| | | $C_2S$ | | $(Ca_{2,00}Mg_{0,03}Mn_{0,02})_{2,05}(Si_{0,90}A_{10,01}Fe_{0,02})_{0,93}O$ |
| | | CaO | | $(Ca_{0,71}Mg_{0,11}Fe_{0,02}Mn_{0,02})_{0,86}O$ |
| 3 | 10 – 8,5 | Per | 0,05 | $(Mg_{0,93}Fe_{0,05}Mn_{0,01})_{0,99}O$ |
| | | Mer | | $Ca_{3,12}(Mg_{0,94}Fe_{0,02})_{0,96}(Si_{1,94}Al_{0,02})_{1,96}O$ |
| 4 | 8,5 – 7 | Per | 0,23 | $(Mg_{0,75}Fe_{0,22}Ca_{0,01}Mn_{0,01}Al_{0,01})_{1,00}O$ |
| | | Mf | 0,72 | $(Mg_{1,00}Ca_{0,08}Mn_{0,07})_{1,15}(Fe_{2,51}Ti_{0,02}A_{10,19})_{2,72}O_4$ |
| | | Mer | 0,07 | $Ca_{3,03}(Mg_{0,94}Fe_{0,07})_{1,01}Si_{1,92}O_8$ |
| | | CaMf*[1] | 0,69 | $(Ca_{0,57}Mg_{0,72}Mn_{0,04})_{1,33}(Fe_{1,62}Ti_{0,02}A_{10,16}Si_{0,23})_{2,03}O_5$ |
| 5 | 7 – 0 | Per | 0,30 | $(Mg_{0,68}Mn_{0,01}Fe_{0,30}A_{10,01})_{1,00}O$ |
| | | Mf | 0,70 | $(Mg_{1,06}Ca_{0,07}Mn_{0,06})_{1,19}(Fe_{2,49}Al_{0,09}Si_{0,01})_{2,59}O_4$ |
| | | CaMf | 0,87 | $(Mg_{0,41}Ca_{0,47}Mn_{0,03}Fe_{0,08})_{0,99}(Fe_{2,68}A_{10,13})_{2,81}O_4$ |
| | | $C_2S$ | | $(Ca_{1,90}Mg_{0,02}Na_{0,01})_{1,93}(Si_{0,83}Fe_{0,07})_{0,90}O_4$ |

*[1] CaMg — calicum-rich magnesioferrite.

In reaction zones 4 and 5 the ratio of components abruptly changes within ~7 mm, which is manifested in a perceptible increased content of Fe arriving from the melt. This leads to nearly complete replacement of periclase by magnesioferrite. At the same time, the content of magnesium and calcium migrating from the refractory into the melt via diffusion decreases.

The calculation of the phase norm along the zones of sample M2 generally corroborates the quantitative ratios obtained using optical and electron microscopes. Thus, the amount of periclase toward the contact zone decreases from 90 to 11% and the content of iron oxides in it grows to 30%. Calcium silicates are present in all zones: bicalcium silicate (from 4 to 11.5%) in zones 1, 2, and 5 with the ratio $(CaO/SiO_2) > 2$ and mervinite formed in zones 3 and 4 with the ratio < 2 (in the amount of 15 and 6%, respectively).

In all zones we observed accumulation of Al compared to the initial content, but it is more perceptible in the first two zones (> 4.5 $Al_2O_3$), which is presumably related to the reaction between the refractory ramming and the underlying chamotte mixture. Calcium aluminate formed in these zones comprises 6.2 and 10.2%, respectively. The increasing content of iron oxide toward the contact zone raises the quantity of the wustite component in periclase to 30% and leads to its replacement by magnesioferrite (up to 78% in zone 5). The free lime content decreases toward the contact and completely disappears in zone 3, having become part of the silicates.

The concentration of titanium decreases and that of manganese monotonically grows while approaching the contact with metallurgical melts.

The skeleton, banded, and cellular structures formed by magnesioferrite and calcium silicate crystals suggest that they emerge in crystallization of the melt arising between the relict periclase grain aggregates. The diffusion substitution process changes the composition, so that the formation of a ferrous melt that is in equilibrium with magnesioferrite and wustite becomes possible in zone 5. This assumption agrees with the data on the $MgO–Fe_2O_3$ system [6] at a temperature above 1600°C indicating the possibility of a melt coexisting with magnesioferrite and wustite.

The change in the phase composition of the material at the zone boundaries is generally corroborated by x-ray phase analysis. The refractory in the zones remote from the contact contains mainly periclase, bicalcium silicate, and lime, whereas the most altered zones contain high-ferrous periclase, magnesioferrite in the form of a magnesioferrite-magnetite solid solution, bicalcium silicate, and x-ray-amorphous phases. Silicate glass has not been identified using the electron microscope but has been observed in polished sections.

## CONCLUSION

A study of the wear of refractories as a consequence of corrosion caused by the chemical interaction between two media, i.e., a refractory material and molten metal and slag, has been performed. The main result is identifying a zonality which regularly arises in all parts of the furnace hearth. The same type of zonality evolves along the refractory material, regardless of its grade. The meaning of this zonality is the variation in the chemical composition of the refractory in the solid state, as a result of mutual diffusion of the components of two contrasting media and, accordingly, regular variations of the paragenesis of the minerals (phases) upon moving from the hearth toward the refractory — melt interface. The general trend of the refractory composition variations in the same direction is as follows: an increasing content of Fe, a decreasing content of Mg and Ca, replacement of calcium aluminates by silicates (bi- and tricalcium), sometimes by mervinite instead of tricalcium silicate, the emergence of calcium ferrite, and the growing role of iron oxides. One of the most significant results is the emergence of the wustite (or magnesioferrite) melt in the zone of the most intense interaction between the refractory and the metallurgical slag. This phenomenon is a negative factor, since the emergence of the melt facilitates the erosion of the upper layer of the refractory. The process of evolution of the melt over the solid phases (the melt substitution) is related to the changes in the chemical composition and is fundamentally different from melting. Recrystallization in the presence of the melt is responsible for the skeleton form of the crystalline material persisting in this zone. The ability of the emerging melt to separate from crystals and keep flowing results in its segregation as bands and drops, decreases its volume in cooling, and leads to the formation of larger pores and cavities, which reduces the resistance of the refractory.

We believe that capillary impregnation, which is considered one of the main factors of destruction of refractories, does not occur here to a significant extent, but the most probable reason for the formation of the melt in the refractory is the chemical reactions between the components in the course of mutual diffusion between two contrasting media.

The study of the valence state of iron in refractories demonstrated that iron in the least altered zone has mainly the bivalent form. In the most altered zone, the content of iron oxides significantly grows and that of the trivalent form becomes nearly twice the bivalent form, which shows that the reducing conditions have been replaced by more oxidizing ones. Mineralogically, trivalent iron is mainly identified in magnesioferrite, magnetite, and calcium ferrite.

Another factor believed to be negative for a refractory is the presence of bicalcium silicate [7]. One of the reasons for the formation of $Ca_2SiO_4$ is the increased concentration of $SiO_2$ in the refractory mixture and a low $CaO/SiO_2$ ratio. However, it has been found that bicalcium silicate is present in the zone closest to the contact with metallurgical melt in all samples, regardless of the initial composition (grade) of the refractory. In the near-contact zones its content is not more than 5 – 7% and it exists in paragenesis with iron oxides or spinellides (FeO or $MgFe_2O_4$). It is presumably present in a liquid state during the furnace operation, similar to

part of the Fe compounds. In numerous samples we have identified phosphor and magnesium (fractions of a percent) in $Ca_2SiO_2$, which are known to have a stabilizing crystallochemical effect. Therefore, it can be assumed that the presence of $Ca_2SiO_4$ in a refractory does not affect its destruction.

However, the rather high content of Ca in the initial refractory mixtures (the factor of increased activity of Ca) should be regarded as a necessary condition for the stability of refractories, since precisely Ca is capable of binding silica (as calcium silicates) that arrives from metallurgical melts to the refractory mixture and preventing the formation of higher-melting silicates. The comparison of Jehearth and Ankerharth refractories indicates that their chemical and mineral compositions after service and formation of zonality are very similar, despite the difference in their initial compositions (with respect to Ca and Mg). This is responsible for their similar physicotechnical parameters which determine the high resistance of both refractories in steel melting.

## REFERENCES

1. T. I. Shchekina, E. N. Gramenitskii, A. M. Batanova, et al., "Use of magnesian-dolomite mixtures in steel-melting furnace hearths and the mechanism of their wear in service. 1. Study of Ankerhearth refractories," *Nov. Orneupory*, No. 10, 45 – 54 (2006).
2. *Materials from Slovakian Magnesite Works JSC*, Elshava, Slovakia.
3. R. E. Muan, "Phase equilibria in the system CaO–MgO–iron oxide at 1500°C," *J. Am. Ceram. Soc.*, **48**(7), 359 – 364 (1965).
4. V. Ekshtein, A. Krontaler, and M. Zinbernagle, "ANKERHATH mixtures for arc furnaces: refractories for the future," *Nov. Ogneupory*, No. 4, 51 – 54 (2005).
5. Phase ratios in $FeO–Fe_2O_3–MgO$ system, in: *Minerals: a Reference Book. Phase Equilibrium Diagrams* [in Russian], Nauka, Moscow (1974).
6. B. Phillips, "Phase equilibria in the system $MgO–Fe_2O_3$," *J. Am. Ceram. Soc.*, **44**(4), 169 (1961) (*Minerals: a Reference Book. Phase Equilibrium Diagrams* [in Russian], Nauka, Moscow (1974)).
7. A. P. Nagornyi, "Stabilization of the elements of work space lining in open-hearth furnaces," *Ogneupory Tekh. Keram.*, No. 5, 36 – 39 (1997).